Acta Pharmaceutica Sinica B 2024;14(10):4345–4359

Chinese Pharmaceutical Association
Institute of Materia Medica, Chinese Academy of Medical Sciences

Acta Pharmaceutica Sinica B

www.elsevier.com/locate/apsb
www.sciencedirect.com

ORIGINAL ARTICLE

Amylovis-201 is a new dual-target ligand, acting as an anti-amyloidogenic compound and a potent agonist of the σ_1 chaperone protein

Laura García-Pupo [a,#], Lucie Crouzier [b], Alberto Bencomo-Martínez [a], Johann Meunier [b], Axelle Morilleau [b], Benjamin Delprat [b], Marquiza Sablón Carrazana [a], Roberto Menéndez Soto del Valle [a], Tangui Maurice [b,*], Chryslaine Rodríguez-Tanty [a,*]

[a]*Department of Neurochemistry, Cuban Center for Neurosciences, Cubanacan, Playa, Havana CP 11600, Cuba*
[b]*MMDN, University of Montpellier, EPHE, INSERM, Montpellier 34095, France*

Received 19 March 2024; received in revised form 12 April 2024; accepted 4 June 2024

KEY WORDS

Alzheimer's disease;
Amyloid-β aggregation;
Neuroprotection;
σ_1 receptor;
Drug discovery;
Molecular modelisation;
Zebrafish model;
Learning and memory

Abstract The aggregation of Amyloid-β (Aβ) peptides is associated with neurodegeneration in Alzheimer's disease (AD). We previously identified novel naphtalene derivatives, including the lead compound Amylovis-201, able to form thermodynamically stable complexes with Aβ species, peptides and fibrils. As the drug showed a chemical scaffold coherent for an effective interaction with the σ_1 receptor chaperone and as σ_1 agonists are currently developed as potent neuroprotectants in AD, we investigated the pharmacological action of Amylovis-201 on the σ_1 receptor. We report that Amylovis-201 is a potent σ_1 agonist by several *in silico*, *in vitro* and *in vivo* assays and that its anti-amnesic and neuroprotective effects involve a pharmacological action at σ_1 receptors. Furthermore, we show for the first time that classical σ_1 receptor agonist (PRE-084), and antagonist (NE-100) are able to interact and disaggregate Aβ_{25-35} fibrils. Interestingly, Amylovis-201 was the only compound inhibiting Aβ_{25-35} aggregates formation. Our results therefore highlight a dual action of Amylovis-201 as anti-aggregating agent and σ_1 receptor agonist that could be highly effective in long-term treatment against neurodegeneration in AD.

*Corresponding authors.
E-mail addresses: tangui.maurice@umontpellier.fr (Tangui Maurice), chris@cneuro.edu.cu (Chryslaine Rodríguez-Tanty).
[#]Present address: Laboratory of Protein Science, Proteomics and Epigenetic Signaling (PPES), Department of Biomedical Sciences, University of Antwerp, 2610 Wilrijk, Belgium.
Peer review under the responsibility of Chinese Pharmaceutical Association and Institute of Materia Medica, Chinese Academy of Medical Sciences.

https://doi.org/10.1016/j.apsb.2024.06.013

1. Introduction

Despite the progress achieved by drug discovery programs, the availability of disease-modifying therapies for Azheimer's disease (AD) is limited. Among the different reasons for this, one is that developing drugs directed to only one therapeutic target might not be sufficient to tackle a multifactorial neurodegenerative disorder, such as AD[1]. Amyloid-β (Aβ) peptide oligomerization and deposition are pathological hallmarks of AD-related neurodegeneration[2]. Also, Aβ accumulation impairs mitochondrial proteostasis[3,4] and the expression of tethering proteins which connect the endoplasmic reticulum (ER) with mitochondria[5,6].

The sigma-1 (σ_1) receptor is a highly conserved transmembrane protein expressed in the ER membrane of several different cell types. By its chaperoning activity, the σ_1 receptor interacts with other proteins and modulates calcium flux and the ER stress response[7,8]. Interestingly, the σ_1 receptor shows druggable features, and several small compounds have been characterized as agonists, positive modulators, as well as antagonists (extensively reviewed by Vavers et al.[9] and Maurice[10]). Substantial *in vivo* preclinical data show that σ_1 agonists are potent anti-amnesic and neuroprotective compounds in neurodegenerative diseases, such as AD, Parkinson's disease, amyotrophic lateral sclerosis, and Huntington's disease[11]. In fact, some σ_1 agonists, notably blarcamesine (ANAVEX2-73) and pridopidine are evaluated at phase 2/3 clinical trials for AD and Huntington disease, respectively[10].

In our previous work, we have designed a new family of naphthalene derivatives, called Amylovis, which form stable complexes with Aβ peptides and inhibit its aggregation *in vitro*. Furthermore, the lead compound Amylovis-201 (CNEURO-201) also decreases the Aβ burden in the brain of triple transgenic AD mice and improves their cognitive performance[12]. The Amylovis compounds carry in their structures an amidoalkylic chain with different terminal functional groups, which make them versatile candidates not only for AD therapy, but also as imaging diagnosis systems[13]. Interestingly, structural similarities exist between the chemical scaffold of Amylovis compounds and the pharmacophore of σ_1 agonists[10,14]. Moreover, Amylovis compounds induce anti-amnesic and neuroprotective effects, which resemble the well-known pharmacological activity of σ_1 receptor agonists. Hence, we here evaluated the potential activity of the lead compound Amylovis-201 as a σ_1 receptor ligand. First, our *in silico* predictions and cell-based *in vitro* results show that Amylovis-201 is a potent σ_1 agonist. Second, using *in vivo* σ_1 receptor-mediated responses, we show that Amylovis-201 acts as an anti-amnesic and neuroprotective drug in the mouse and zebrafish models, through its σ_1 agonist activity. Altogether, we demonstrated that Amylovis-201 has a unique dual activity as Aβ anti-aggregation and neuroprotective σ_1 agonist. The drug is a promising neuroprotectant for AD by promoting Aβ clearance and cellular cytoprotection.

2. Materials and methods

2.1. *In silico studies*

2.1.1. *Molecular docking*

All ligand−protein molecular docking simulations were performed with the AutoDockVina program (Vina)[15]. The partial charges of the ligands were calculated using the Gasteiger model[16]. The nonpolar hydrogen atoms were fused to the heavy atoms. In ligands, the rotatable bonds were maintained by default with the help of the TORSDOF tool from AutoDockTools[17]. The structures of the protein (PDB code 5HK1), and the amyloid-β_{25-35} peptide (PDB code 1QXC) remained rigid, while that of the ligands remained flexible. The computation was carried out with the use of configuration files (one file for each of the desired simulations) which preferentially use the Vina parameters. One hundred results were obtained. These results were subjected to a clustering process and 2.0 Å was used as the tolerance value. To select the amino acids that interact with each ligand, 4.6 Å is used as cut-off distance. All contacts that repeated in 85% or more of all obtained solutions are considered to be included in the interaction zone.

2.1.2. *Molecular dynamic simulations*

The physicochemical properties (parameters) of the non-protein ligands were obtained from the Generalized Amber Force Field[18]. For each ligand the partial atomic charges were calculated using the semi-empirical method AM1-BCC (antechamber subroutine), which is implemented in the AMBER program (University of California San Franscisco, CA, USA)[19]. For the assignment of the ligand charges, the one that is present in its structure at a pH value of 7.4 was chosen. In each system, the parameters corresponding to the protein were generated with the AMBER99SB force field. The energy minimization procedure was performed with GROMACS v4.6.5 package (University of Groningen, The Netherlands)[20]. Hydrogen atoms were added to the starting structures, using the protonation states predicted above. A dodecahedron was created as a solvation box for each complex, with a distance between the solute surface and the box walls of 10 Å. Water molecules were then added using the explicit solvent model TIP3P[21]. Simulations of each complex were performed under periodic boundary conditions. The temperature at which all systems were run was 310 K.

2.2. *Drugs*

The σ_1 receptor antagonist 4-methoxy-3-*N*,*N*-dipropylbenzeneethanamine (NE-100) was obtained from Tocris (Tebu-Bio). 2-(4-Morpholinethyl)-1-phenylcyclohexane carboxylate hydrochloride (PRE-084) and (5*S*,10*R*)-(+)-5-methyl-10,11-dihydro-5*H*-dibenzo[*a*,*d*]cyclohepten-5,10-imine hydrogen maleate ((+)-MK-801, Dizocilpine) were from Sigma−Aldrich (Saint-Quentin-Fallavier, France). (*E*)-*N*-(Cyclopropylmethyl)-*N*-ethyl-3,6-diphenylhex-5-en-3-amine (JO-1784, Igmesine) was from Pfizer (Fresnes,

France). Methyl (2-{[4-(1-naphthylamino)-4-oxobutanoyl]amino} ethyl)dithiocarbamate (Amylovis-201) was synthesized as previously described[12]. Amyloid β-[25−35] fragment ($A\beta_{25-35}$) was from Eurogentec (Angers, France) and dissolved in distilled water at 3 mg/mL and stored at −20 °C until use.

2.3. *In vitro binding of [^{3}H](+)-pentazocine to σ_1 receptor*

The assay was performed by CEREP (Celle l'Evescault, France). Increasing concentrations of PE-084 or Amylovis-201 (0.1 nmol/L to 10 μmol/L) were incubated with 15 nmol/L of [^{3}H](+)-pentazocine in membranes preparations from Jurkat human leukemic T cells. Samples were incubated during 120 min at 37 °C and non-specific binding level was determined using 10 μmol/L of haloperidol. Assays were performed in duplicates and results were expressed as % of specific binding level.

2.4. *σ_1 protein-BiP dissociation assays*

The activity of Amylovis-201 as σ_1 agonist was evaluated as its ability to dissociate the ER stress chaperone BiP from the σ_1 receptor in σ_1-overexpressing cells[8]. Green fluorescent protein (GFP)-tagged σ_1 protein-overexpressing Chinese hamster ovarian (CHO) cells, kindly provided by Drs Tsung-Ping Su and Yukio Kimura (NIDA, NIH, Baltimore, MD, USA), were expanded in minimum essential medium culture medium supplemented with 10% heat-inactivated fetal bovine serum and 2 mmol/L Glutamax (Invitrogen, Carlsbad, CA, USA). After plating the cells, different concentrations of each compound were added for 30 min (37 °C) and then the culture medium was replaced by phosphate buffered saline (3 mL). The cells were harvested and suspended in 50 mmol/L Hepes pH 7.4, then cross-linked with 50 μg/mL of dithiobissuccinimidyl propionate (Thermoscientific, Waltham, MA, USA). The reaction was terminated by adding Tris/HCl 50 mmol/L pH 8.8. After incubating 15 min on ice, the cells were lysed in 50 mmol/L Tris pH 7.4 buffer, containing 150 mmol/L NaCl, 1% Triton X-100, 0.3% sodium deoxycholate, 0.1% sodium dodecylsulfate, and protease inhibitor cocktail (Roche Applied Science, Basel, Switzerland). After centrifugation at 16,000×*g* for 1 min, the supernatant was incubated with Chromotek GFP-trap agarose (Proteintech, United Kingdom) overnight at 4 °C. After centrifugation at 16,000×*g* for 1 min, the supernatant was discarded and the pellet was suspended in 0.5 mL buffer (50 mmol/L Tris (pH 7.4), 150 mmol/L NaCl, 1% Triton X/100, 0.3% sodium deoxycholate, 0.1% SDS), rinsed twice, and analyzed by Heat Shock 70 KDa Protein 5 ELISA assay (#CL-SEC343Mu, Euromedex, Souffelweyersheim, France).

2.5. *Light scattering assay*

The light scattering assay was conducted as described[8] but adapted in 96 well-plate, with a reaction volume of 200 μL. Aliquots of the amyloid-β[25−35] peptide ($A\beta_{25-35}$) (Eurogentec, Angers, France) were dissolved in hexafluoroisopropanol (Merck, France) to avoid aggregation, dried before kinetic experiment, and solubilized in 100% dimethyl sulfoxide (DMSO, Merck, France). Aliquots of 80 mL of peptide stock solution were diluted in 120 mL of 10 mmol/L Tris buffer pH = 7.5 (270 mmol/L final concentration of peptide), then kinetic experiment was immediately launch by using microplate reader (Multiskan Sky, Thermoscientific, France) at a wavelength of 350 nm for 2 h. Absorbance was measured every minute. Amylovis-201, NE-100, or PRE-084 were dissolved in DMSO and either added, at a stoichiometric ratio of 1:1 (270 mmol/L), at t = 0 min to see their effect on peptide aggregation, or, at a stoichiometric ratio of 1:1 or 1:2, at t = 60 min to see their effect on peptide disaggregation. Experiments were performed in triplicates. Data were analyzed by using Prism software (GraphPad, v10.0, GraphPad Software, San Diego, CA, USA) by calculating the area under curve.

2.6. *Cytotoxicity induced by $A\beta_{25-35}$ in neuroblastoma cells*

Human neuroblastoma SH-SY5Y cells were routinely cultured in Dulbecco's modified Eagle's medium (Gibco, France), supplemented with 10% fetal bovine serum (Gibco, France). Aliquots of $A\beta_{25-35}$ solubilized in water were incubated at 37 °C for 4 days to allow complete oligomerization of the peptide. The compounds (Amylovis-201, PRE-084 and NE-100) were dissolved in dimethylsulfoxide (DMSO) and further diluted in cell growth medium. To initiate the experiments, the cells were seeded in 96 wells-plates at a density of 10,000 cells/well and were incubated at 37 °C and 5% CO_2 for 24 h. Then, different concentrations of the compounds (Amylovis-201 and PRE-084) were added to the cells simultaneously with aggregated $A\beta_{25-35}$, with or without the presence of the σ_1 antagonist NE-100. After 24 h of incubation, the cell viability was indirectly determined by the 3-(4,5-dimethylthiazol-2-yl)-2,5-diphenyltetrazolium bromide (MTT) assay (CyQuant MTT cell viability assay, ThermoFisher, France), following the manufacturer recommendations.

2.7. *Zebrafish breeding and drug treatments*

Mutant *wfs1ab*^{KO} and wild-type *wfs1ab*^{WT} zebrafish lines were generated and maintained as previously described[22]. Briefly, zebrafish lines were maintained in an automated fish tank system (ZebTEC, Tecniplast) at 28 °C, pH 7, conductivity around 500 μS and with a 14 h:10 h light:dark cycle. They were fed with standard diet. Embryos were collected from natural breeding, raised at 28.5 °C in E3 medium (5 mmol/L NaCl, 0.17 mmol/L KCl, 0.33 mmol/L $CaCl_2$, 0.33 mmol/L $MgSO_4$).

At 5 dpf, individual larvae are transferred in wells of 96 well plate (Whatman #7701-1651 square and flat bottom wells) with 300 μL embryo medium and placed in the incubator at 28 °C. The *wfs1ab*^{WT} larvae were placed in even wells and *wfs1ab*^{KO} in odd wells. Larvae that did not have swim bladders or presented visible physiological deformities were not used for the experiment. The Amylovis-201 drug was dissolved in DMSO and was applied at three different concentrations to the larvae (1−3 μmol/L).

2.8. *Visual motor response*

The visual motor response (VMR) assay quantifies the locomotor activity of zebrafish larvae in response to light changes using infrared (IR) tracking system. The experiments were performed as described[22]. Briefly, at 5 dpf, the locomotor behavior of larvae was monitored by using an automated video tracking device (Zebrabox, ViewPoint), employing a DinionXF 1/3-inch Monochrome camera (model BFLY-PGE-13H2M, FLIR) fitted with a fixed-angle megapixel lens (SR5014MP-5C, Seiko Optical). In the device, larvae in 96-well plate are isolated from environmental surrounding noise. The box floor emitted by a light-controlling unit a white light (69−83 μW/cm^2 measured at λ 495 nm). The response to stimuli

was recorded by an IR camera (25 frames/s) under IR light illumination at 850 nm, which the animals could not perceive.

The experiment started at 10:00 am and consisted in acclimating larvae to darkness (0% brightness) for 30 min, then switching light ON (100% brightness) for 10 min, then OFF (0% brightness) during 10 min. This was repeated twice, giving a total experiment duration of 70 min. The brightness changes were immediate (<< 1 s). The detection sensitivity was set to 31, activity burst threshold to 30 and activity freeze threshold to 10. Locomotor activity between the two threshold values was considered as normal activity. The distance covered was measured in mm/s. The values obtained in OFF were subtracted for each larvae to their ON values in order to normalize with the basic locomotion for each larvae.

2.9. Mice breeding and drug treatments

Male OF1 inbred mouse of 3 months old of age were maintained in the animal facility of the University of Montpellier (CECEMA) for experiments. Animals were housed in group, allowed food and water *ad libitum* access except during experiments. They were maintained in a controlled environment (22 ± 1 °C, 55 ± 5% humidity) with a 12 h:12 h light/dark cycle, lights on at 7:00 h. Behavioral testing was performed between 10:00 and 16:00 h. All animal procedures were conducted in strict adherence to the European Union Directive 2010/63 and ARRIVE guidelines[23] and authorized by the national ethic committee (Paris) (APAFIS# 35307-2022020909546393).

PRE-084 and NE-100 were solubilized in physiological saline (vehicle solution). Amylovis-201 was solubilized in Cremophor (Sigma−Aldrich), then brought up to 10% in saline. It was administered intraperitoneally (ip) or, *per os* by gavage (*po*), in accordance with the design of each experiment, at the indicated doses in a volume of 5 mL/kg body weight, 30 min before the behavioral tests. Before administration, Aβ_{25-35} oligomerization was performed by incubating the peptide at 37 °C for 4 days. Intracerebroventricular (icv) injections were performed as previously described and control injections were included with the vehicle solution (distilled water)[24].

2.10. Spontaneous alternation in the Y-maze

The spatial working memory of the mice was evaluated as from the spontaneous alternation in the Y maze[24-26]. The maze was made of grey polyvinylchloride. Each arm was 40 cm long, 13 cm high, 3 cm wide at the bottom, 10 cm wide at the top, and converging at an equal angle. Each mouse was placed at the end of one arm and allowed to move freely through the maze during an 8 min session. The series of arm entries, including possible returns into the same arm, was recorded visually. An alternation was defined as entries into all three arms on consecutive occasions. The number of maximum alternations was therefore the total number of arm entries minus two and the percentage of alternation was calculated as Eq. (1):

$$\text{Percentage of alternation (\%)} = (\text{Actual alternations}/\text{Maximum alternations}) \times 100 \quad (1)$$

Animals that failed to explore more than 8 arms in 8 min were removed from the calculations.

2.11. Step-through passive avoidance

The contextual non-spatial long term memory was studied by the step-through passive avoidance test as previously described[27]. The apparatus is a two compartment (15 cm × 20 cm × 15 cm high) box with one illuminated with white polyvinylchloride walls and the other darkened with black polyvinylchloride walls and a grid floor. A guillotine door separates each compartment. A 60 W lamp positioned 40 cm above the apparatus lights up the white compartment during the experiment. Scrambled foot shocks (0.3 mA for 3 s) could be delivered to the grid floor using a shock generator scrambler (Lafayette Instruments, Lafayette, USA). The guillotine door was initially closed during the training session. Each mouse was placed into the white compartment. After 5 s, the door was raised. When the mouse entered the darkened compartment and placed all its paws on the grid floor, the door was closed and the foot shocks delivered for 3 s. The step-through latency, that is the latency spent to enter the darkened compartment, and the shock sensitivity (estimated as 0 = no reaction, 1 = flinching reactions, 2 = flinchings and vocalizations) were recorded. None of the treatment affected shock sensitivity (data not shown). The retention test was performed 24 h after training. Each mouse was placed again into the white compartment. After 5 s, the door was raised. The step-through latency was recorded up to 300 s each. Results were expressed as median and interquartile (25%−75%) range because the data are nonparametric with an established upper limit.

2.12. Statistical analyses

Analyses were done using Prism v10.0. Data were analyzed using one-way analysis of variance (ANOVA, F value) or two-way ANOVA with genotype and treatment as independent variables, followed by a Dunnett's test. Passive avoidance latencies, expressed as median and interquartile range and represented as box-and-whiskers, were analyzed using a nonparametric Kruskal−Wallis ANOVA (H value) and *post hoc* comparisons done using the Dunn's test.

3. Results

3.1. Amylovis-201 interaction with the σ_1 protein

Glennon et al.[14] described a pharmacophore model of the σ_1 protein binding pocket that present simple requirements for optimal binding: a proton donor amine is flanked by a distal primary hydrophobic region and by a proximal secondary hydrophobic regions, both able to form hydrophobic interactions within the binding pocket (Fig. 1a). Amylovis-201 only partially responds to this requirement as the molecule presents the nitrogen atom with the distal hydrophobic naphthalene ring. However, the proximal dithiocarbamate group is more hydrophilic and cannot support Glennon's predicted interactions (Fig. 1a). Using the [^{3}H](+)-pentazocine binding assay in membranes preparations from Jurkat human leukemic T cells, we observed that PRE-084 inhibited the S1R radiotracer binding with a K_i of 42 nmol/L (Fig. 1b) but Amylovis-201 failed to show any inhibition at concentrations up to 10 μmol/L (Fig. 1b).

However, to further investigate a possible interaction of the Amylovis-201 with the σ_1 protein, we performed molecular

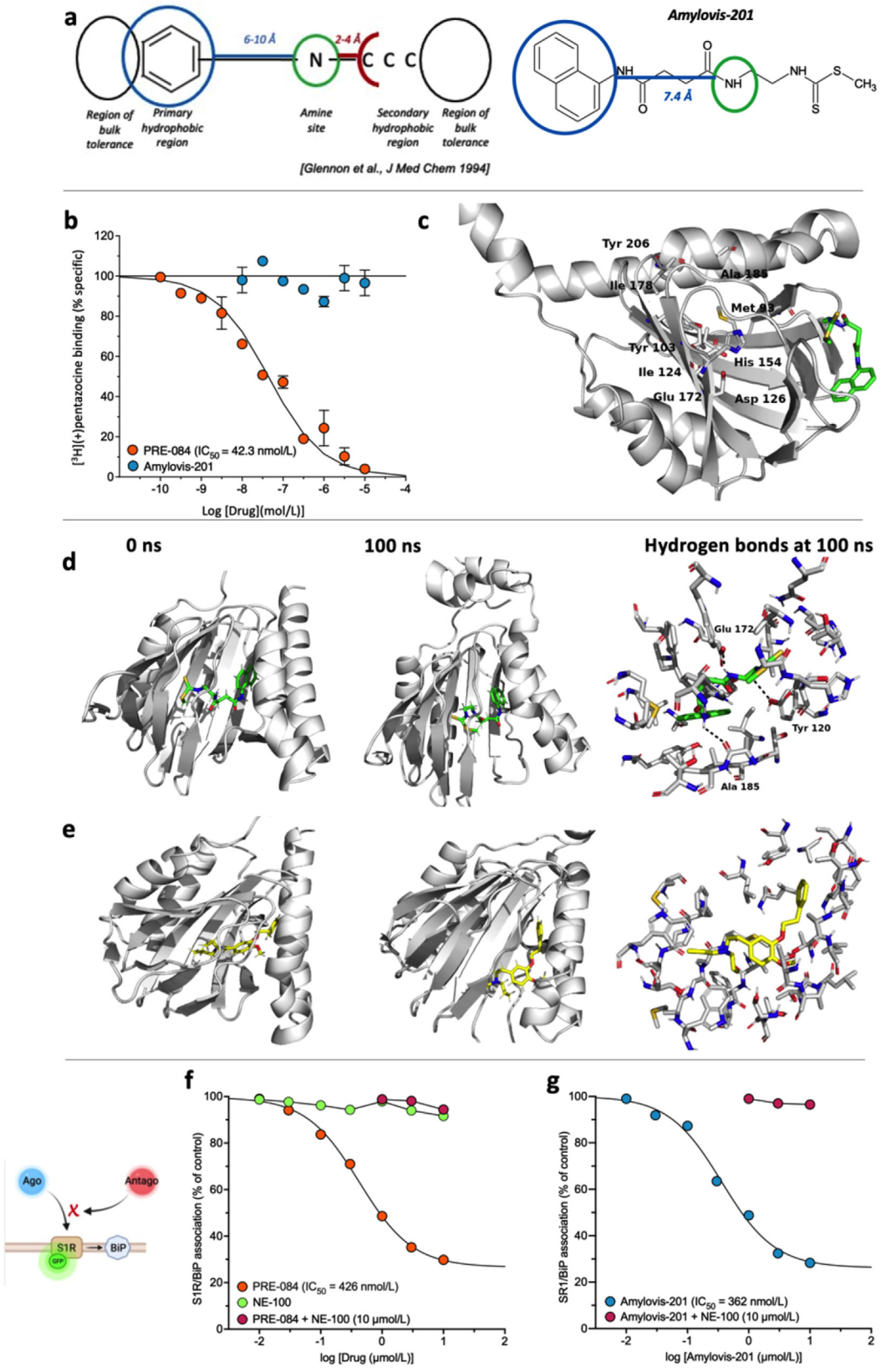

Figure 1 Amylovis-201 is a σ_1 receptor interacting drug. (a) Pharmacophore structure proposed by Glennon et al.[14] and application to the developed formula of Amylovis-201. Note that the secondary hydrophobic region does not fit with the hydrophilic dithiocarbamate part. (b) Inhibition of (+)-[^{3}H]pentazocine specific binding to Jurkat human leukemic T cells by PRE-084 and Amylovis-201. (c) Amino acids identified in the ligand binding pocket (LBP) of the σ_1 protein and which are critical for ligand-protein interactions. In the 3D model of the protein, the LBP is profoundly occluded within the protein and unreachable for Amylovis-201. Molecular dynamics were performed between 0 and 100 ns with (d)

docking and dynamic simulations. We used the subunit b of the 5HK1 protein as implemented in Pascual et al.[28] from the crystallized structure[29]. The simulation area comprised the amino acids: Tyr206, Leu182, Ile178, Glu172, Ile124, His154, Asp126, Leu105, Val84, Ala185, Met93 and Tyr103 (Fig. 1c), as described by Pascual et al[28]. The ligand binding pocket (LBP) appeared to be deeply embedded inside the protein. In this condition when the LBP is occluded, Amylovis-201 could not interact with the key amino acids due to a structural impediment in the protein that prevents the compound penetration into the cavity (Fig. 1c). However, the σ_1 protein conformation likely changes depending on activation[30,31] and also involves the interaction with BiP co-chaperone[8]. Therefore, we analyzed further the binding requirements of Amylovis-201 and compared them with the prototypic ligands NE-100, a reference σ_1 antagonist, and PRE-084, a reference σ_1 agonist. When considering the crystallized structure of the σ_1 protein with the antagonist compound NE-100 (PDB code 6DK0) we identified hydrophobic interactions, between the electronic clouds of the phenyl rings with the side chains of the amino acids Tyr103 and Tyr206, and van der Waals interactions, between the terminal part of the ligand and His154 (Supporting Information Fig. S1a). No hydrogen bond interaction was observed in the complex formed. However, some polar attractive and/or repulsive interactions could be expected due to the O atoms present in the ligand structure. The molecular docking model was able to reproduce these interactions with a 0.5 Å difference between the position of the ligands, and similar hydrophobic and van der Waals interactions were observed as those found in the 6HK0 crystal structure (Fig. S1b). The interaction zone of PRE-084 showed mostly hydrophobic $\pi-\pi$ interactions towards the phenyl group (Fig. S1c). The ligand established hydrophobic interactions with the side chains of the amino acids Tyr103 and Tyr206. This type of interaction seems to be essential in drugs with a Glennon-type structure, which may be related to the stability of the complex formed and to the specific function they perform in the protein. Noteworthy, similar results were obtained with the other selective σ_1 agonist igmesine (Fig. S1d). Moreover, it must be noted that, in all the simulations performed, the interaction with His154 was lost for each agonist.

In the case of Amylovis-201, the molecular docking simulations showed that the ligand behavior was very similar to that of NE-100 or PRE-084, analyzed so far (Fig. S1e). Amylovis-201 indeed showed $\pi-\pi$ type hydrophobic interaction between the electronic cloud of the naphthalene group and the side chain of the amino acid Tyr103. A van der Waals interaction between the C═S double bond region of Amylovis-201 and His154 was also observed (Fig. S1e). In addition, the positively charged nitrogen atom, central to the Glennon pharmacophore, appeared capable of forming electrostatic interactions with Glu172. These interactions probably allowed the rearrangement of the rest of the molecule and achieved its stability through hydrophobic interactions[32]. Note that when the molecular docking of structures NE-100, PRE-084 and Amylovis-201 are superposed, the orientation of the three ligands is very close with the only difference regarding Amylovis-201 being the H-bonds to amino acids Glu172 and Ile124 (Fig. S1f). In addition, molecular dynamics simulations show the formation of three hydrogen bonding interactions with the H atoms of the NHCX (X = O or S) groups of the Amylovis-201 compound and the O atoms of the COO^- groups of Glu172 (2.1 Å), Ala (2.7 Å) and Tyr (2.7 Å), which presumably provide enhanced stability to the formed complex (Fig. 1d and Supporting Information Fig. S2). This type of interaction was not observed in any of the other previous ligands nor in the crystallographic structure with NE-100.

Molecular docking and dynamic simulations therefore suggested that Amylovis-201, if penetrant, could interact with the σ_1 protein. To examine whether the drug could show a σ_1 activity in physiological condition, we used the σ_1 protein/BiP dissociation assay in a cellular preparation. After activation, the σ_1 protein dissociates from the ER heat shock protein 70 (Hsp70) family member BiP[8] and this response is now used as a specific σ_1 activity test *in vitro*. We used GFP-tagged σ_1 protein-overexpressing CHO cells, immunoprecipitation and ELISA assays. As shown in Fig. 1f, the treatment with PRE-084 caused a dose-dependent dissociation of σ_1 protein from BiP with an IC_{50} of 426 nmol/L. The treatment with NE-100, at concentrations up to 10 μmol/L, did not affect σ_1 protein/BiP association. However, the combined treatment between NE-100 and the highest three doses of PRE-084 abolished the PRE-084-induced σ_1 protein/BiP dissociation (Fig. 1f). Amylovis-201 also acted as an inducer of σ_1 protein/BiP dissociation with an even higher efficacy than PRE-084 since it showed an IC_{50} value of 362 nM (Fig. 1g). The activity of Amylovis-201 was completely blocked by a co-treatment with NE-100 at 10 μmol/L, which demonstrated its σ_1 receptor agonist activity (Fig. 1g). We concluded that, although we failed to determine a binding affinity of Amylovis-201 for the σ_1 receptor, the drug has the ability to bind to the protein, as predicted by molecular docking and dynamic simulation studies. Indeed in a cell-based assay, the compound behaved as a potent σ_1 agonist.

3.2. *Amylovis-201 attenuated σ_1 protein related behavioral dysfunctions in zebrafish and mouse models*

3.2.1. *Attenuation of the hyperlomocotor response in wolframin mutant zebrafish larvae*

Following functional *in vitro* assays, we evaluated the *in vivo* activity of Amylovis-201 in animal models in which the treatment with σ_1 receptor agonists is known to improve behavioral impairments. We recently showed that selective σ_1 receptor agonists restored the functionality of ER-mitochondria Ca^{2+} exchanges and resulting behavioral alterations in animal models of Wolfram syndrome[22]. In particular, they attenuated the hyperlocomotor response of *wfs1ab*^{KO} zebrafish larvae in the VMR assay.

As expected, untreated *wfs1ab*^{KO} zebrafish larvae showed a hypermobility pattern in the visual motor response as compared with the *wfs1ab*^{WT} line (Fig. 2a and b). The treatment with increasing concentrations of Amylovis-201 in the water bath resulted in a U-shaped dose-dependent decrease of the

Amylovis-201 and (e) NE-100. H-bonds are shown as dashed lines at 100 ns (f) PRE-084 dissociated BiP from σ_1 protein in GFP-tagged σ_1 protein-overexpressing CHO cells with an IC_{50} value of 426 nmol/L. NE-100 failed to do so at concentrations up to 10 μmol/L, but, at 10 μmol/L, prevented the dissociating effect of PRE-084. (g) Amylovis-201 dissociated BiP from σ_1 protein with an IC_{50} of 362 nmol/L. Its effect was blocked by NE-100. Experiments were performed in duplicates.

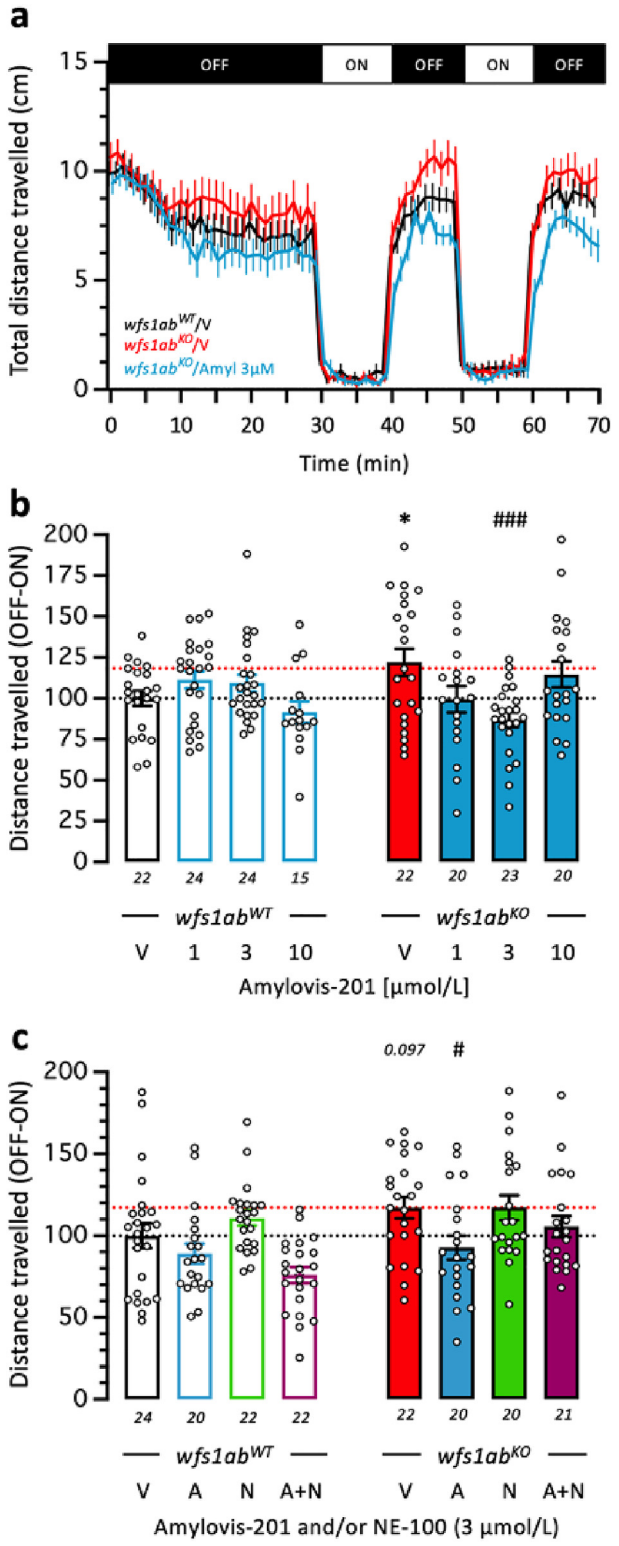

Figure 2 Amylovis-201 attenuated the hyperlocomotor response of 5 dpf*wfs1ab*^{KO} mutant zebrafish larvae in the VMR test through σ_1 agonism: (a) VMR activity profiles of V-treated *wfs1ab*^{WT}and *wfs1ab*^{KO} mutant lines and *wfs1ab*^{KO} zebrafish treated with Amylovis-201 at 3 µmol/L; (b) dose−response effect of Amylovis-201 on the zebrafish mobility; and (c) effect of NE-100. The fish mobility was measured for 70 min, with 30 min of training in the dark (OFF), then 2 cycles of light/dark (ON/OFF) of 10 min each. In (b, c), the distance traveled by w*fs1ab*^{WT} and *wfs1ab*^{KO} larvae during the light/dark cycle was averaged as differences between the OFF and ON phases. Data show mean ± SEM of the number of animals indicated below the columns. Two-way ANOVAs: $F_{(1,162)} = 0.4218$, $P = 0.5170$ for the genotype, $F_{(3,162)} = 1.316$, $P = 0.2710$ for the treatment, $F_{(3,162)} = 5.561$, $P = 0.0012$ for the interaction in (b); $F_{(1,163)} = 9.608$, $P = 0.0023$ for the genotype, $F_{(3,63)} = 6.781$, $P = 0.0002$ for the treatment, $F_{(3,163)} = 1.616$, $P = 0.1876$ for the interaction in (c). $^{*}P < 0.05$ *vs.* V-treated *wfs1ab*^{WT} zebrafish; $^{\#}P < 0.05$, $^{\#\#\#}P < 0.001$ *vs.* V-treated *wfs1ab*^{KO} zebrafish; Dunnet's test.

hyperlocomotor response, with a complete restoration at 3 µmol/L (Fig. 2a and b). Amylovis-201 treatment had no effect on the visual motor response of the control *wfs1ab*^{WT} line (Fig. 2b). The combined treatment with the σ_1 receptor antagonist NE-100 (3 µmol/L) attenuated the Amylovis-201 effect in the *wfs1ab*^{KO} zebrafish larvae, as no significant difference with the vehicle-treated *wfs1ab*^{KO} larvae was observed (Fig. 2c). It must be noted that the co-treatment with NE-100 and Amylovis-201 significantly decreased the normal visual motor response in control *wfs1ab*^{WT} line (Fig. 2c), which suggested that the drug combination may not be devoid of effect by itself in the fish.

3.2.2. *Attenuation of dizocilpine-induced learning deficits in mice*

The acute treatment with dizocilpine, a noncompetitive antagonist of the glutamatergic *N*-methyl-D-aspartate (NMDA) receptor, induces a significant alteration of memory that was repeatedly shown to be alleviated by selective σ_1 receptor agonists[25,26,33].

The pre-treatment with Amylovis-201 significantly attenuated the dizocilpine-induced alternation deficits, at the doses of 0.03 and 0.1 mg/kg in a bell-shaped manner (Fig. 3a). Importantly, Amylovis-201 did not affect the dizocilpine-induced hyperlocomotion of mice, in the 0.01−0.1 mg/kg dose range but only at the highest dose tested (Fig. 3b), showing that the observed *in vivo* pharmacological effects of Amylovis-201 are selectively related to cognitive rather than motor responses. In the long-term contextual memory test, dizocilpine significantly altered the passive avoidance response (Fig. 3c), an effect that was attenuated by 0.1 or 1 mg/kg Amylovis-201. The attenuation, however, remained non-significantly different from the response of (dizocilpine + vehicle)-treated animals (Fig. 3c).

The co-treatment with NE-100 at 1 mg/kg IP, blocked the amelioration of dizocilpine-induced spontaneous alternation deficits promoted by Amylovis-201 at 0.03 mg/kg *po* (Fig. 3d), and the increase in step-through latency induced by Amylovis-201 at 0.1 mg/kg *po* (Fig. 3e). These observations showed that Amylovis-201 behaved as a σ_1 receptor agonist in the modulation of spatial working memory and contextual long-term memory processes in mice.

3.2.3. *Amelioration of the Aβ_{25-35}-induced learning impairment in mice*

The σ_1 receptor agonists were identified as neuroprotectant in AD in the pharmacological mouse model induced by ICV administration of oligomerized Aβ_{25-35}[27,34]. Amylovis-201 was therefore tested in Aβ_{25-35}-treated mice and the drug prevented the spontaneous alternation deficits at 1 and 3 mg/kg ip (Fig. 4a), with no effect on locomotion in Aβ_{25-35}-treated mice (Fig. 4b). It also attenuated the passive avoidance impairments at the highest dose

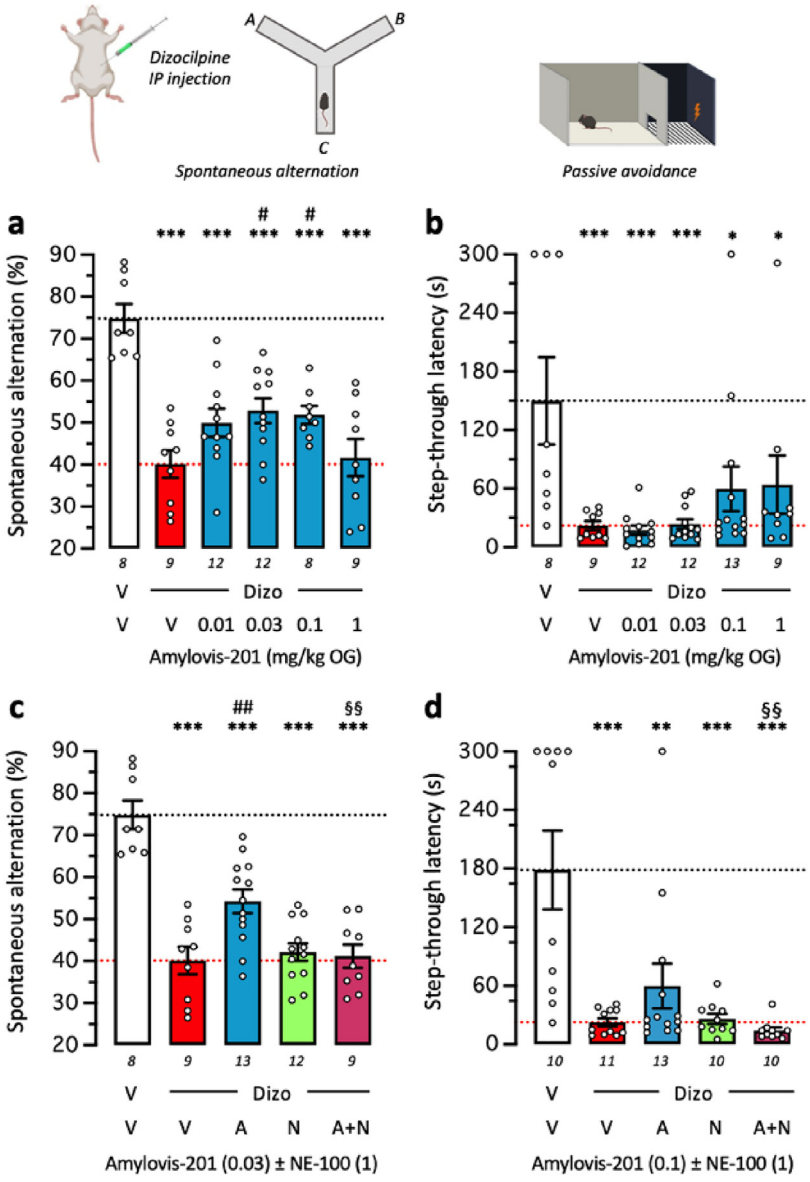

Figure 3 Amylovis-201 attenuated Dizocilpine-induced learning impairment in mice through σ_1 agonism: dose-response effects in the (a) spontaneous alternation and (b) step-through passive avoidance. (c,d) Blockade of Amylovis-201 effect by NE-100 in each test. Mice received Amylovis-201 (0.01−1 mg/kg PO) 10 min before Dizocilpine (0.15 mg/kg IP), 20 min before the Y-maze session in (a,c) or passive avoidance training in (b,d). In (c,d), NE-100 was administered at 1 mg/kg IP simultaneously with the lowest active dose of Amylovis-201, *i.e.*, 0.03 mg/kg PO in the Y-maze in (d) and 0.1 mg/kg in the passive avoidance test in (e). Abbreviations: V, vehicle solution (physiological saline); Dizo, Dizocilpine; A, Amylovis-201; N, NE-100. Data show mean ± SEM of the number of animals indicated within or below the columns. ANOVAs: $F_{(5,50)} = 12.19$, $P < 0.0001$ in (a); $F_{(4,46)} = 22.76$, $P < 0.0001$ in (c). Kruskal-Wallis ANOVAs: $H = 19.29$, $P = 0.0017$ in (b); $H = 23.86$, $P < 0.0001$ in (d). * $P < 0.05$, ** $P < 0.01$, *** $P < 0.001$ *vs.* (V+V)-treated mice; $^{\#}$ $P < 0.05$, $^{\#\#}$ $P < 0.01$ *vs.* (Dizo+V)-treated mice; ^{oo} $P < 0.01$ *vs.* (Dizo+A)-treated mice; Dunnett's test in (a,c), Dunn's test in (b,d).

tested (Fig. 4c). In addition, a pretreatment with the σ_1 receptor antagonist NE-100 (3 mg/kg ip) prevented both effects on spontaneous alternation (Fig. 4c) and passive avoidance (Fig. 4d) induced by the highest dose of Amylovis-201. The data showed that Amylovis-201 behaved *in vivo* as a σ_1 receptor agonist with anti-amnesic and neuroprotective potentials at low doses in the mg/kg range.

Finally, Amylovis-201 has been shown to prevent Aβ-induced cytotoxicity *in vitro*[12]. In order to evaluate whether this effect is related to the anti-aggregating effect or to the σ_1 receptor agonist activity of the compound, we evaluated its effect in SH-SY5Y cells exposed to a toxic (25 µmol/L) concentration of $A\beta_{25-35}$. As expected, the treatment with oligomeric $A\beta_{25-35}$ induced a significant decrease in the viability of human neuroblastoma cells (Fig. 4e). The combined treatment with the σ_1 antagonist NE-100 (3 or 10 µmol/L) eliminated the neuroprotective effect of Amylovis-201, the S1R antagonist having no effect by itself or on $A\beta_{25-35}$-induced toxicity (Fig. 4e). The data suggested that the σ_1 receptor agonist activity of Amylovis-201 is markedly involved in its acute neuroprotective activity.

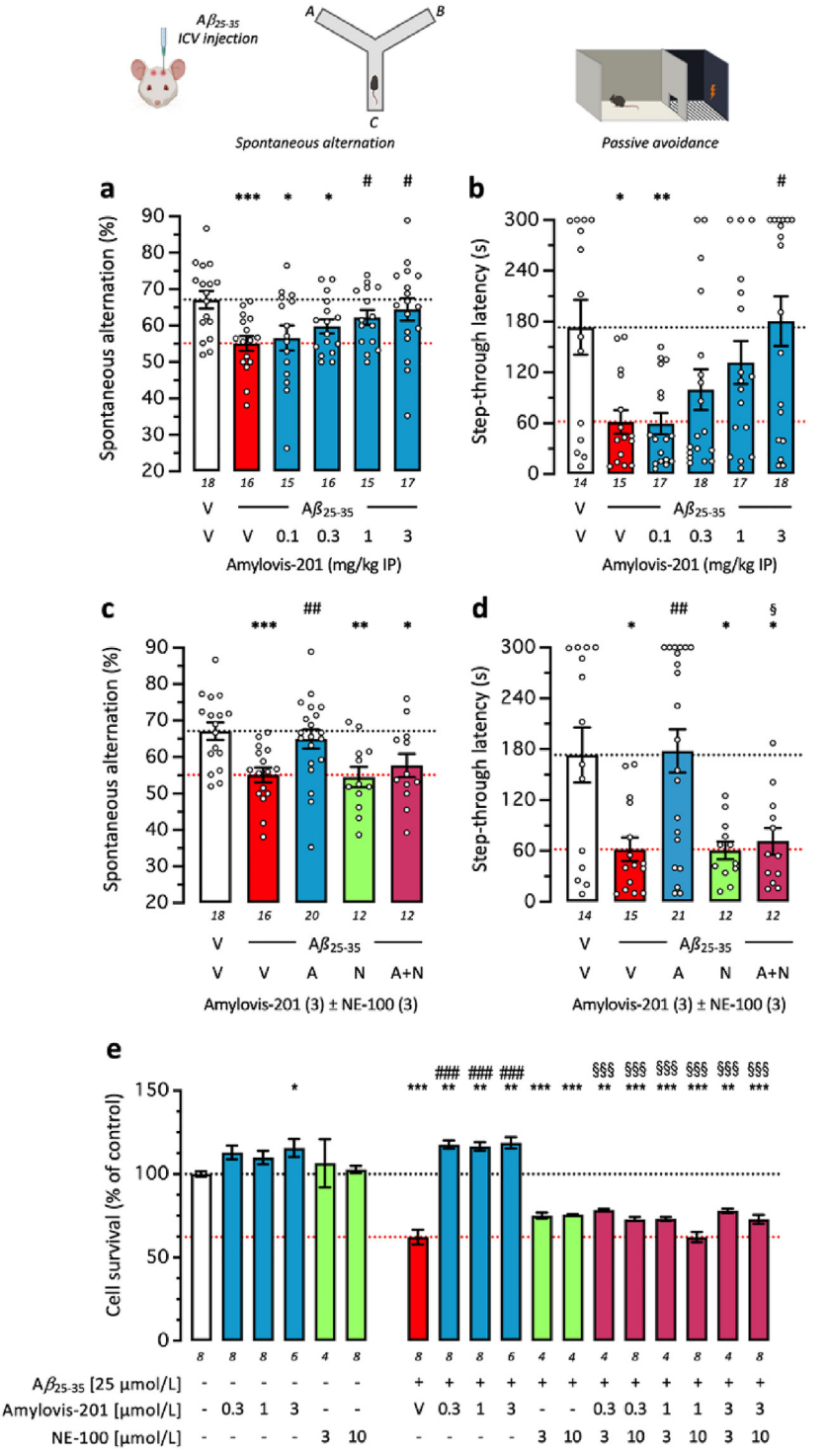

Figure 4 Amylovis-201 attenuated Aβ_{25-35}-induced learning impairment in mice and Aβ_{25-35}-induced cytotoxicity in SH-SY5Y cells through σ_1 agonism: dose−response effects in the (a) spontaneous alternation in the Y-maze and (b) step-through passive avoidance. (c, d) Blockade of Amylovis-201 effect by NE-100 in each test. Mice received oligomerized Aβ_{25-35} peptide (9 nmol, icv) or vehicle solution and then Amylovis-201 (0.3−3 mg/kg ip) 7 days before behavioral analyses. The Y-maze session was performed on Day 7 (a, c) and passive avoidance training on Day 8 and retention on Day 9 (b, d). In (c, d), NE-100 was administered at 3 mg/kg ip simultaneously with Amylovis-201 at 3 mg/kg IP. (e) SH-SY5Y neuroblastoma cells (10,000 cells/well) were exposed to Aβ_{25-35} (25 µmol/L) and Amylovis-201 (0.3−3 µmol/L) and/or NE-100 (3, 10 µmol/L). Cell survival was monitored after 24 h using the MTT assay. Abbreviations: V, vehicle solution (physiological saline); A, Amylovis-201; N, NE-100. Data show mean ± SEM of the number of determination indicated within or below the columns. ANOVAs: $F_{(5,90)} = 3.336$, $P = 0.0082$ in (a); $F_{(4,72)} = 5.109$, $P = 0.0011$ in (c); $F_{(11,80)} = 49.51$, $P < 0.0001$ in (e). Kruskal−Wallis ANOVAs: $H = 13.5$, $P = 0.0019$ in (b); $H = 14.18$, $P = 0.007$ in (d). $^{*}P < 0.05$, $^{**}P < 0.01$, $^{***}P < 0.001$ *vs.* (V + V)-treated mice or untreated cells; $^{\#}P < 0.05$, $^{\#\#}P < 0.01$, $^{\#\#\#}P < 0.001$ *vs.* (Aβ_{25-35}+V)-treated mice or cells; $^{\S}P < 0.05$, $^{\S\S\S}P < 0.001$ *vs.* (Aβ_{25-35} +Amylovis-201)-treated mice or cells; Dunnett's test in (a, c, e), Dunn's test in (b, d).

3.3. *Anti-aggregating effect of Amylovis-201 and σ_1 receptor ligands*

Amylovis-201 was shown to present numerous interactions like H-bonds, electrostatic and $\pi-\pi$ stackings, in the N- and C-terminal regions of Aβ protein that led to effective prevention of its aggregation, as confirmed using thioflavine fluorescence experiments in human microglia SV-40 cell line[12]. In molecular docking studies with peptide Aβ_{25-35} and NE-100, PRE-084 and Amylovis-201, it was observed that Amylovis-201 presented a strong hydrophobic interaction with the amino acids Ala30, Ile31, Ile32 and Gly33 (Fig. 5a) as did NE-100 (Fig. 5b) and PRE-084 (Fig. 5c). However, in contrast to the other compounds, three hydrogen bonds are observed in Amylovis-201 (Fig. 5a). These are formed between the H and O atoms of the NHCO group of the amidoalkyl chain of the compound and the O and H atoms of the COO and OH groups of Ser26 (2.1 and 2.8 Å), respectively. Similarly, an H-bond is formed between the H atom of the NHCSS group of the compound and the O atom of the $CONH_2$ group of Asn27 (2.3 Å). These three bonds should confer greater stability to the complex formed. To clarify whether this anti-aggregating effect was unrelated to the σ_1 receptor activity of the drug, we compared Amylovis-201, PRE-084 and NE-100 in a light scattering assay, as used to demonstrate the chaperone activity of the σ_1 protein itself[8]. The Aβ_{25-35} fragment was used as it shares with longer A$\beta_{1-40/42}$ proteins the ability to aggregate and induce toxicity[35], and bears one of the interacting domains for Amylovis-201[12]. Furthermore, Aβ_{25-35} fragment was used in the *in vivo* and *in vitro* experiments in this study. When Aβ_{25-35}, 270 mmol/L, initially in a hexafluoroisopropanol-soluble form, was placed in water it spontaneously aggregated with a half-time of approximately 10 min (Fig. 5d). Co-incubation with a 1:1 stoichiometry with Amylovis-201 fully prevented the increase in OD, so the spontaneous Aβ_{25-35} aggregation, confirming the potent anti-aggregating effect of the compound (Fig. 5d). As the naphthalene moiety of the compound is responsible for most of the interactions with Aβ protein, and as it constitutes a major requirement of Glennon's pharmacophore for effective binding to the σ_1 protein, we investigated whether other σ_1 compounds could directly interact with Aβ_{25-35} aggregation. Co-incubation with PRE-084 or NE-100 failed to affect Aβ_{25-35} aggregation (Fig. 5e). Moreover, we also tested whether the compounds can promote disaggregation of Aβ oligomers. They were added at a stoichiometry of 1:1 or 1:2, 1 h after Aβ_{25-35} when the light scattering plateau value is reached. Amylovis-201 rapidly decreased the light scattering level: −57% at 1:1, and −86% at 1:2, after 1 h (Fig. 5f). PRE-084 and NE-100, at 1:1, allowed a significant decrease in optic density, by −33% and −30% after 1 h, respectively (Fig. 5g). However, increasing the concentration, with the 1:2 stoichiometry for PRE-084, failed to increase the disaggregation level (Fig. 5g). These data showed that although the chemical structure of σ_1 receptor ligands presented characteristics that could specifically interfere with Aβ aggregation and particularly promote Aβ disaggregation, Amylovis-201 is more potent to prevent Aβ aggregation *de novo* and as a disaggregating agent.

4. Discussion

Due to the multifactorial nature and long-time progression of AD, novel drug design and development campaigns in the last decade focused on pleiotropic drugs directed toward different molecular targets[1,36,37]. Furthermore, several theranostics are being developed to improve brain targeting across the blood−brain barrier (BBB) and the early diagnosis of the disease[38,39]. We previously showed that, Amylovis-201, the lead compound of a new family of naphthalene derivatives crossed the BBB and targeted Aβ deposits[13]. Amylovis compounds are neuroprotective against different *in vitro* neuronal stress conditions, such as apoptosis[40,41]. Moreover, Amylovis-201 inhibited Aβ aggregation and counteracted Aβ deposition and cognitive dysfunctions in a triple transgenic mouse model of AD[12]. Amylovis-201 has also been evaluated in a model of neuronal deterioration induced by ICV administration of streptozotocin, where it was observed that daily oral administration of Amylovis-201 reduced the loss of hippocampal neurons and improved spatial memory[42]. In this study, we confirmed the ability of Amylovis-201 to interact and inhibit the aggregation of amyloid proteins, namely Aβ_{25-35}, and to protect against the cytotoxicity induced by Aβ_{25-35} in neuroblastoma cells. More importantly, we investigated the potential pharmacological activity of Amylovis-201 to act as a σ_1 receptor ligand.

The σ_1 protein is a unique therapeutic target due to its dual nature as a molecular chaperone and as a ligand-operated receptor[8,10,43-46]. It regulates several cellular signaling pathways in normal and diseased states[45-47] by interacting with numerous partner proteins notably expressed in the functional contacts between mitochondria and ER, called mitochondria-associated ER membranes (MAMs)[8,43], the plasma membrane[46,48,49], and the nuclear envelope[50,51]. The result of the σ_1 protein activity is to release or associate with partner proteins allowing them to relocalize or to become activated[43,45,46]. However, the protein was also identified as a receptor, since it bears numerous pharmacological hallmarks of it. Indeed, small drugs can activate the σ_1 protein, thus behaving as agonists or positive modulators, or preventing its activation, and behaving as an antagonist or negative modulator (for reviews[9,10]). The pharmacophore has been described, initially from binding studies and then confirmed and improved by successive structural biology and crystallographic studies[14,28,29,52]. From the σ_1 structural data, all the proposed pharmacophore models coincide in an essential positive ionizable group, a basic amino group most often represented by a nitrogen atom, flanked by two hydrophobic regions at defined spatial distances[14,28,52-57]. Interestingly, the chemical scaffold of Amylovis-201 includes a naphthalene group monosubstituted by an amido alkyl chain with a terminal dithiocarbamate group that partly responded to Glennon's pharmacophore model. However, the drug failed to show a significant inhibition of (+)[^{3}H]-pentazocine binding at concentrations of 10 μmol/L. Molecular docking and dynamic simulations helped to better understand whether and how Amylovis-201 might interact with the σ_1 receptor. Based on the crystallographic structure of the σ_1 protein, molecular docking analyses with NE-100, PRE-084 and Amylovis-201 revealed that the latter could interact with the same amino acids within the LBP of the σ_1 protein, notably by establishing hydrophobic interactions of the $\pi-\pi$ type with the side chains of the amino acids Tyr103 and Tyr206. This type of interaction is essential in all drugs with a Glennon-type structure as they are related to the stability of the complex formed and to the specific function they perform in the protein. Amylovis-201, however, did not present the secondary hydrophobic domain but rather interacted efficiently with His154 through van der Waals interactions between its C=S double bond region and the amino acid. These two types of interactions are coherent with previous reports[28]. Moreover, the nitrogen atom considered as the center of Glennon's pharmacophore is able to

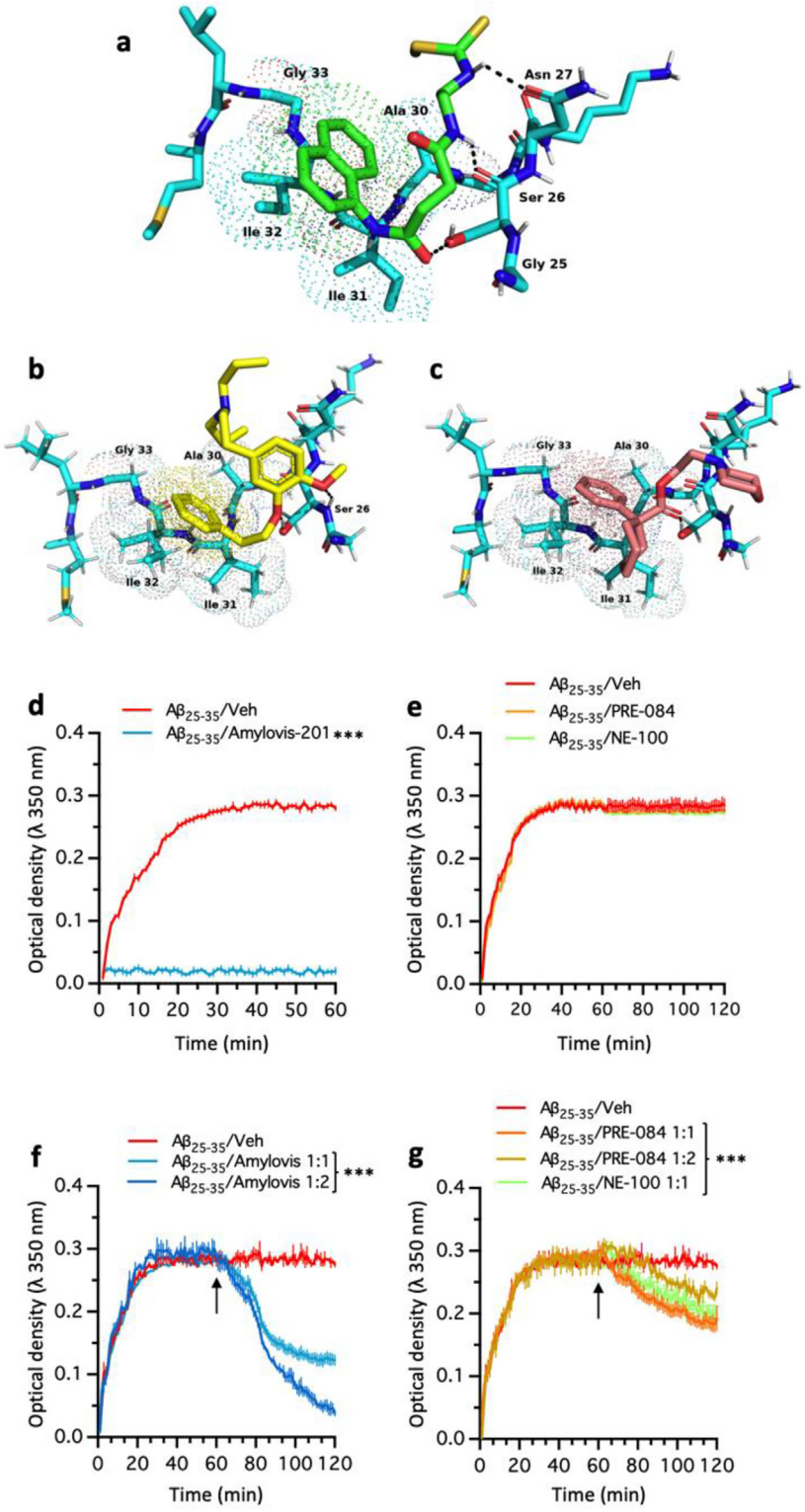

Figure 5 Amylovis-201 anti-aggregating properties *in vitro*. Molecular docking with Aβ_{25-35} peptide. Molecular rigid docking models of the complexes (stick representations): (a) Amylovis-201-Aβ_{25-35} peptide; (b) NE-100-Aβ_{25-35} peptide; (c) PRE-084-Aβ_{25-35} peptide. The Aβ_{25-35} amyloid peptide code used 1QXC (PDB). (d) Light scattering of Aβ_{25-35} (25 µmol/L in 40 mmol/L HEPES, pH 7.4) spectrophotometrically monitored at 43 °C in absence or presence of Amylovis-201. Numbers in parentheses indicate molar ratios of proteins. (e) Light scattering of Aβ_{25-35} in absence or presence of PRE-084 or NE-100. (f) Light scattering of Aβ_{25-35} when Amylovis-201, PRE-084 or NE-100 were added after 1 h at a stoichiometry 1:1. (g) Same experiment with a stoichiometry1:2. Experiments were performed in triplicates.

form hydrogen bonds with the amino acid Glu172. These interactions were also described by Pascual et al.[28] with the lead compounds in their study as salt bridge formation between the ligand and the protein. In our case, these are two hydrogen bonding interactions which presumably provide greater stability to the complex formed. This type of interaction was not observed in any of the other previous ligands or in the crystallographic structure obtained with NE-100[32]. These structural features seemed suitable for effective binding to σ_1 protein. Indeed, by using a cellular assay, the ligand-induced σ_1 protein/BiP dissociation in CHO cells[8], we were able to show a cellular activation of the σ_1 protein by Amylovis-201 with an IC_{50} value even lower to that of the reference σ_1 agonist PRE-084 (362 *vs*. 426 nmol/L). These observations therefore questioned the fact that Amylovis-201 failed to inhibit (+)[^{3}H]-pentazocine binding. Recent studies, and our present data, coherently showed that the LBP is, when the σ_1 protein is in its native form as a homomeric trimer[32], very profound within the 3D structure of the protein and almost occluded. Interestingly, Rossino et al.[31] recently reported bitopic σ_1 ligands able to simultaneously bind to a peripheral site on the cytosol-exposed surface that stabilizes the open conformation of the σ_1 protein, and to the occluded primary binding site, triggering the σ_1 activity. This very elegant demonstration of the direct impact of ligands on the σ_1 protein conformation for optimal binding and activity may explain several atypical features known about the σ_1 protein and not fully explained. In particular, several very active compounds *in vivo* only present poor σ_1 binding affinity. These compounds are weakly linear and rather compact molecules that may not be able to penetrate and reach the LBP. In homogenate membrane preparations, they might be unable to adequately bind the σ_1 protein. However, in cellular and *in vivo* experiments, the σ_1 protein is likely in a different conformational/activation state, putatively through endogenous activation that can be allowed by several physiological signals, such as local ER changes in calcium levels or cellular redox status[8,58]. This physiological conformation may lead to the opening of the occluded primary binding site and allow molecules responding to the Glennon's pharmacophore requirements but unable to reach the LBP, to exert their σ_1 activity. Although further studies are needed, our results suggest that some compounds, less effective in reaching the LBP, may be more effective *in vivo* than their expected binding affinity. In fact, this is often the case for several small compounds. For example, neurosteroids, such as dehydroepiandrosterone and pregnenolone, show a poor micromolar affinity to inhibit (+)[^{3}H]-pentazocine binding but acted as σ_1 protein agonists at low doses *in vivo* (mg/kg range) in learning and memory tests[59-61]. A second example is blarcamesine, a drug in clinical stage in AD, that showed a higher target occupancy than PRE-084 in positron emission tomography with the highly selective σ_1 radioligand [^{18}F]FTC-146 in the rodent brain although its σ_1 binding affinity is much lower (K_i of 896 nmol/L *vs*. 44 nmol/L)[62,63]. We therefore propose that Amylovis-201 is a third example for this kind of molecules for which the standard binding assay, using (+)[^{3}H]-pentazocine or other reference σ_1 radioligand, and a protocol based on a classical membrane homogenate preparation and standard buffer conditions, could fail to determine a binding potency to σ_1 receptors that appear coherent with its ability to act as a potent σ_1 agonist in cellular or *in vivo* conditions.

Indeed, we confirmed the potent activity of Amylovis-201 as a σ_1 receptor agonist by using several *in vivo* responses known to engage in σ_1 activity. First, we reported the suitability to target the σ_1 receptor in the Wolfram syndrome, a rare genetic disease due to a mutation of wolframin, a MAM resident protein that, when altered, disrupts calcium transfer from the ER into the mitochondria and provokes a MAMopathy[22]. The σ_1 receptor was validated as a therapeutic target particularly in a zebrafish line, *wfs1ab*^{KO}, which showed a hyperlocomotor response in the VMR test, restored to control levels by overexpression of the σ_1 protein or by active σ_1 agonists[22]. Amylovis-201 improved the visual motor alterations of *wfs1ab*^{KO} zebrafish larvae at a concentration of 3 µmol/L, similarly as reported for PRE-084[22] and in a NE-100 sensitive manner, hence by a mechanism involving the activation of the σ_1 receptor.

It is known σ_1 agonists potently attenuate the learning deficits induced by dizocilpine, the NMDA receptor antagonist[25,26,33] and this is considered as a direct behavioral consequence of the ability of σ_1 protein to positively modulate the NMDA receptor activation[47,64]. Amylovis-201 was able to attenuate, for the passive avoidance response, or significantly prevent, for the spontaneous alternation response, the dizocilpine-induced short- and long-term memory deficits, in a NE-100-sensitive manner. This observation confirmed not only that the compound behaved *in vivo* as a σ_1 agonist but also that it appeared more potent than the reference compound PRE-084. Also, Amylovis-201 showed active doses of 0.03 and/or 0.1 mg/kg depending on the test. These doses are ten times lower than our observations with PRE-084 in the same procedures[26].

We also explored the ability of Amylovis-201 to protect against Aβ_{25-35}-induced learning deficits, which is a suitable model to show the σ_1 component in donepezil induced pharmacological activity[27] and to characterize the neuroprotective activity of blarcamesine[65-67]. Amylovis-201 prevented the onset of learning and memory deficits in Aβ_{25-35}-treated mice at the dose of 1 and/or 3 mg/kg in the spontaneous alternation and passive test. These effects were completely prevented by a co-treatment with NE-100. The result was expected as previous studies showed an efficacy of the drug in 3xTg-AD mice[12], but revealed a role of the σ_1 receptor in this neuroprotective effect. Noteworthy, the treatment in 3xTg AD mice was a daily dose of 1 mg/kg for eight weeks, but in this study Aβ_{25-35} mice were treated acutely on the day of the ICV injection of Aβ_{25-35}[27].

This set of experiments demonstrated that Amylovis-201 behaved as a potent σ_1 receptor agonist *in vivo*. This pharmacological action must be considered in the mode of action of the drug particularly as concerns its neuroprotective ability. Previous experimental results demonstrated the neuroprotective activity of σ_1 agonists against *in vivo* Aβ neurotoxicity. For instance, PRE-084 exerted cytoprotective[68], mitoprotective[66,69] and anti-amnesic[26] effects in preclinical models of Aβ neurotoxicity. Furthermore, the activation of the σ_1 receptor by PRE-084 protected the BBB integrity in a mouse model of Aβ_{1-42}-neurotoxicity by increasing the expression of endothelial tight junction proteins, vascular endothelial growth factor (VEGF) and the low-density lipoprotein receptor-related protein 1 (LRP-1)[70]. Interestingly, the endothelial receptor LRP-1 regulates the endosomal transcytosis of Aβ at the BBB, promoting its clearance from the brain to the blood[70,71]. Altogether the results suggested that σ_1 activation decrease the soluble and insoluble A$\beta_{40/42}$ deposits in the hippocampus of AD mice by enhancing their clearance from the brain.

Yet another mechanism by which activated σ_1 protein activity might influence the brain amyloid burden is the direct chaperoning of Aβ peptides, inhibiting their aggregation. The σ_1 protein

interacts with partner protein and inhibits their ability to aggregates. This was shown for citrate synthase, brain-derived neurotrophic factor, insulin, and low-density lipoproptein[8]. We previously observed that purified σ_1 protein was able to interact with several Aβ peptides, including Aβ_{1-42} and Aβ_{25-35}, and inhibit their spontaneous aggregation in a cell-free environment (unpublished data). Other authors recently demonstrated that the σ_1 agonist pridopidine potentiated the inhibitory effect of the σ_1 protein on purified citrate synthase aggregation[51]. Furthermore, the stabilization of σ_1 protein in the small oligomers state by agonists[30,72] might favor the interaction of σ_1 and Aβ peptides, therefore inhibiting Aβ aggregation. Our light scattering results confirmed that Amylovis-201 is able to: (1) fully prevent Aβ aggregation *de novo* and (2) completely disaggregate Aβ, in a concentration-dependent manner. This effect was mildly shared by other σ_1 receptor ligands, like PRE-084 or NE-100, as they failed to prevent Aβ aggregation and significantly but partially (25%) induced Aβ disaggregation, without further effect by increasing the concentration. These last set of experiments clearly showed that Amylovis-201 has a specific effect on Aβ aggregation, due to its optimal chemical structure for an effective interaction with the β-sheets in Aβ aggregates.

Finally, we confirmed the neuroprotective effect of Amylovis-201 in a cell culture model and showed that the protection induced by a short-term application of the drug, during 24 h, is mainly due to the σ_1 receptor agonist activity as it was fully prevented by NE-100. However, in chronic treatment protocols in transgenic mouse models of AD, or in long-term clinical use in human patients, the ability of the drug to exert a dual effect on: (1) cytoprotection through its σ_1 agonist activity, and (2) prevention of Aβ aggregation and induction of Aβ disaggregation through its specific structural effect, strongly suggests that the drug will represent a promising novel disease-modifying therapeutic candidate for AD. This study also confirmed that innovative dual-acting ligands could be identified, or intentionally designed *a priori* as in the case of multi-targets directed ligands, that could efficiently address the complexicity of the neurodegenerative processes in complex pathologies such as Alzheimer's disease.

Acknowledgments

This work was supported by a PHC Carlos J. Finlay program from Campus France (project 47069SA) to TM and CRT. The authors thank Drs Tsung-Ping Su and Yukio Kimura (NIDA, NIH, Baltimore, MD, USA) for the gift of GFP-tagged σ1 protein-overexpressing CHO cells, and the CECEMA animal facility of the University of Montpellier and the ZebraSens behavioral phenotyping platform for zebrafish models at MMDN.

Author contributions

Laura García-Pupo: Writing − review & editing, Writing − original draft, Investigation, Formal analysis, Data curation. Lucie Crouzier: Writing − review & editing, Formal analysis, Data curation. Alberto Bencomo-Martínez: Formal analysis, Data curation. Johann Meunier: Formal analysis, Data curation. Axelle Morilleau: Formal analysis, Data curation. Benjamin Delprat: Writing − review & editing, Formal analysis. Marquiza Sablón Carrazana: Writing − review & editing, Formal analysis. Roberto Menéndez Soto del Valle: Writing − review & editing, Formal analysis, Data curation. Tangui Maurice: Writing − review & editing, Writing − original draft, Resources, Project administration, Methodology, Investigation, Funding acquisition, Formal analysis, Data curation, Conceptualization. Chryslaine Rodríguez-Tanty: Writing − review & editing, Writing − original draft, Methodology, Investigation, Formal analysis, Conceptualization.

Conflicts of interest

The authors declare no conflict of interest.

Appendix A. Supporting information

Supporting information to this article can be found online at https://doi.org/10.1016/j.apsb.2024.06.013.

References

1. Frautschy SA, Cole GM. Why pleiotropic interventions are needed for Alzheimer's disease. *Mol Neurobiol* 2010;**41**:392−409.
2. Decourt B, D'Souza GX, Shi J, Ritter A, Suazo J, Sabbagh MN. The cause of Alzheimer's disease: the theory of multipathology convergence to chronic neuronal stress. *Aging Dis* 2022;**13**:37−60.
3. Hansson Petersen CA, Alikhani N, Behbahani H, Wiehager B, Pavlov PF, Alafuzoff I, et al. The amyloid beta-peptide is imported into mitochondria *via* the TOM import machinery and localized to mitochondrial cristae. *Proc Natl Acad Sci U S A* 2008;**105**:13145−50.
4. Sorrentino V, Romani M, Mouchiroud L, Beck JS, Zhang H, D'Amico D, et al. Enhancing mitochondrial proteostasis reduces amyloid-β proteotoxicity. *Nature* 2017;**552**:187−93.
5. Hedskog L, Pinho CM, Filadi R, Rönnbäck A, Hertwig L, Wiehager B, et al. Modulation of the endoplasmic reticulum−mitochondria interface in Alzheimer's disease and related models. *Proc Natl Acad Sci U S A* 2013;**110**:7916−21.
6. Lau DHW, Paillusson S, Hartopp N, Rupawala H, Mórotz GM, Gomez-Suaga P, et al. Disruption of endoplasmic reticulum-mitochondria tethering proteins in post-mortem Alzheimer's disease brain. *Neurobiol Dis* 2020;**143**:105020.
7. Hayashi T, Maurice T, Su TP. Ca^{2+} signaling *via* $sigma_1$-receptors: novel regulatory mechanism affecting intracellular Ca^{2+} concentration. *J Pharmacol Exp Ther* 2000;**293**:788−98.
8. Hayashi T, Su TP. Sigma-1 receptor chaperones at the ER-mitochondrion interface regulate Ca^{2+} signaling and cell survival. *Cell* 2007;**131**:596−610.
9. Vavers E, Zvejniece L, Maurice T, Dambrova M. Allosteric modulators of sigma-1 receptor: a review. *Front Pharmacol* 2019;**10**:223.
10. Maurice T. Bi-phasic dose response in the preclinical and clinical developments of sigma-1 receptor ligands for the treatment of neurodegenerative disorders. *Expert Opin Drug Discov* 2021;**16**:373−89.
11. Maurice T, Goguadze N. Sigma-1 (σ_1) receptor in memory and neurodegenerative diseases. *Handb Exp Pharmacol* 2017;**244**:81−108.
12. Rivera-Marrero S, Bencomo-Martínez A, Orta Salazar E, Sablón-Carrazana M, García-Pupo L, Zoppolo F, et al. A new naphthalene derivative with anti-amyloidogenic activity as potential therapeutic agent for Alzheimer's disease. *Bioorg Med Chem* 2020;**28**:115700.
13. Rivera-Marrero S, Fernández-Maza L, León-Chaviano S, Sablón-Carrazana M, Bencomo-Martínez A, Perera-Pintado A, et al. [^{18}F] Amylovis as a potential pet probe for β-amyloid plaque: synthesis, *in silico*, *in vitro* and *in vivo* evaluations. *Curr Radiopharm* 2019;**12**:58−71.
14. Glennon RA, Ablordeppey SY, Ismaiel AM, el-Ashmawy MB, Fischer JB, Howie KB. Structural features important for $sigma_1$ receptor binding. *J Med Chem* 1994;**37**:1214−9.

15. Trott O, Olson AJ. AutoDock Vina: improving the speed and accuracy of docking with a new scoring function, efficient optimization, and multithreading. *J Comput Chem* 2010;**31**:455−61.
16. Sadowski J, Gasteiger J. From atoms and bonds to three-dimensional atomic coordinates: automatic model builders. *Chem Rev* 1993;**93**: 2567−81.
17. Morris GM, Huey R, Lindstrom W, Sanner MF, Belew RK, Goodsell DS, et al. AutoDock4 and AutoDockTools4: automated docking with selective receptor flexibility. *J Comput Chem* 2009;**30**: 2785−91.
18. Hanwell MD, Curtis DE, Lonie DC, Vandermeersch T, Zurek E, Hutchison GR. Avogadro: an advanced semantic chemical editor, visualization, and analysis platform. *J Cheminform* 2012;**4**:17.
19. Halgren TA, Merck Molecular Force Field V. Extension of MMFF94 using experimental data, additional computational data, and empirical rules. *J Comput Chem* 1996;**17**:616−41.
20. Pronk S, Páll S, Schulz R, Larsson P, Bjelkmar P, Apostolov R, et al. GROMACS 4.5: a high-throughput and highly parallel open source molecular simulation toolkit. *Bioinformatics* 2013;**29**:845−54.
21. Hornak V, Abel R, Okur A, Strockbine B, Roitberg A, Simmerling C. Comparison of multiple Amber force fields and development of improved protein backbone parameters. *Proteins* 2006;**65**:712−25.
22. Crouzier L, Danese A, Yasui Y, Richard EM, Liévens JC, Patergnani S, et al. Activation of the sigma-1 receptor chaperone alleviates symptoms of Wolfram syndrome in preclinical models. *Sci Transl Med* 2022;**14**:eabh3763.
23. Kilkenny C, Browne W, Cuthill IC, Emerson M, Altman DG. NC3Rs Reporting Guidelines Working Group. Animal research: reporting *in vivo* experiments: the ARRIVE guidelines. *Br J Pharmacol* 2010; **160**:1577−9.
24. Maurice T, Lockhart BP, Privat A. Amnesia induced in mice by centrally administered β-amyloid peptides involves cholinergic dysfunction. *Brain Res* 1996;**706**:181−93.
25. Maurice T, Hiramatsu M, Itoh J, Kameyama T, Hasegawa T, Nabeshima T. Behavioral evidence for a modulating role of sigma ligands in memory processes. I. Attenuation of dizocilpine (MK-801)-induced amnesia. *Brain Res* 1994;**647**:44−56.
26. Maurice T, Su TP, Parish DW, Nabeshima T, Privat A. PRE-084, a sigma selective PCP derivative, attenuates MK-801-induced impairment of learning in mice. *Pharmacol Biochem Behav* 1994;**49**: 859−69.
27. Meunier J, Ieni J, Maurice T. The anti-amnesic and neuroprotective effects of donepezil against amyloid β_{25-35} peptide-induced toxicity in mice involve an interaction with the sigma$_1$ receptor. *Br J Pharmacol* 2006;**149**:998−1012.
28. Pascual R, Almansa C, Plata-Salamán C, Vela JM. A new pharmacophore model for the design of sigma-1 ligands validated on a large experimental dataset. *Front Pharmacol* 2019;**10**:519.
29. Schmidt HR, Zheng S, Gurpinar E, Koehl A, Manglik A, Kruse AC. Crystal structure of the human σ_1 receptor. *Nature* 2016;**532**: 527−30.
30. Gromek KA, Suchy FP, Meddaugh HR, Wrobel RL, LaPointe LM, Chu UB, et al. The oligomeric states of the purified sigma-1 receptor are stabilized by ligands. *J Biol Chem* 2014;**289**:20333−44.
31. Rossino G, Rui M, Linciano P, Rossi D, Boiocchi M, Peviani M, et al. Bitopic sigma$_1$ receptor modulators to shed light on molecular mechanisms underpinning ligand binding and receptor oligomerization. *J Med Chem* 2021;**64**:14997−5016.
32. Schmidt HR, Betz RM, Dror RO, Kruse AC. Structural basis for σ_1 receptor ligand recognition. *Nat Struct Mol Biol* 2018;**25**:981−7.
33. Maurice T, Hiramatsu M, Itoh J, Kameyama T, Hasegawa T, Nabeshima T. Low dose of 1,3-di(2-tolyl)guanidine (DTG) attenuates MK-801-induced spatial working memory impairment in mice. *Psychopharmacol Berl* 1994;**114**:520−2.
34. Villard V, Espallergues J, Keller E, Alkam T, Nitta A, Yamada K, et al. Antiamnesic and neuroprotective effects of the aminotetrahydrofuran derivative ANAVEX1-41 against amyloid β_{25-35}-induced toxicity in mice. *Neuropsychopharmacology* 2009;**34**:1552−66.
35. Cotman CW, Anderson AJ. A potential role for apoptosis in neurodegeneration and Alzheimer's disease. *Mol Neurobiol* 1995;**10**:19−45.
36. Lalut J, Santoni G, Karila D, Lecoutey C, Davis A, Nachon F, et al. Novel multitarget-directed ligands targeting acetylcholinesterase and σ_1 receptors as lead compounds for treatment of Alzheimer's disease: synthesis, evaluation, and structural characterization of their complexes with acetylcholinesterase. *Eur J Med Chem* 2019;**162**:234−48.
37. Scheiner M, Hoffmann M, He F, Poeta E, Chatonnet A, Monti B, et al. Selective pseudo-irreversible butyrylcholinesterase inhibitors transferring antioxidant moieties to the enzyme show pronounced neuroprotective efficacy *in vitro* and *in vivo* in an Alzheimer's disease mouse model. *J Med Chem* 2021;**64**:9302−20.
38. Ahmad J, Akhter S, Rizwanullah M, Khan MA, Pigeon L, Addo RT, et al. Nanotechnology based theranostic approaches in Alzheimer's disease management: current status and future perspective. *Curr Alzheimer Res* 2017;**14**:1164−81.
39. Tripathi P, Shukla P, Bieberich E. Theranostic applications of nanomaterials in Alzheimer's disease: a multifunctional approach. *Curr Pharm Des* 2022;**28**:116−32.
40. Fernández-Gómez I, Sablón-Carrazana M, Bencomo-Martínez A, Domínguez G, Lara-Martínez R, Altamirano-Bustamante NF, et al. Diabetes drug discovery: hIAPP1-37 polymorphic amyloid structures as novel therapeutic targets. *Molecules* 2018;**23**:686.
41. Sablón-Carrazana M, Fernández I, Bencomo A, Lara-Martínez R, Rivera-Marrero S, Domínguez G, et al. Drug development in conformational diseases: a novel family of chemical chaperones that bind and stabilise several polymorphic amyloid structures. *PLoS One* 2015;**10**:e0135292.
42. Mercerón-Martínez D, Alacán Ricardo L, Bejerano Pina A, Orama Rojo N, Expósito Seco A, Vega Hurtado Y, et al. Amylovis-201 enhances physiological memory formation and rescues memory and hippocampal cell loss in a streptozotocin-induced Alzheimer's disease animal model. *Brain Res* 2024;**1831**:148848.
43. Hayashi T, Su TP. Sigma-1 receptors (σ_1 binding sites) form raft-like microdomains and target lipid droplets on the endoplasmic reticulum: roles in endoplasmic reticulum lipid compartmentalization and export. *J Pharmacol Exp Ther* 2003;**306**:718−25.
44. Sánchez-Fernández C, Entrena JM, Baeyens JM, Cobos EJ. Sigma-1 receptor antagonists: a new class of neuromodulatory analgesics. *Adv Exp Med Biol* 2017;**964**:109−32.
45. Su TP, Hayashi T, Maurice T, Buch S, Ruoho AE. The sigma-1 receptor chaperone as an inter-organelle signaling modulator. *Trends Pharmacol Sci* 2010;**31**:557−66.
46. Su TP, Su TC, Nakamura Y, Tsai SY. The sigma-1 receptor as a pluripotent modulator in living systems. *Trends Pharmacol Sci* 2016; **37**:262−78.
47. Couly S, Goguadze N, Yasui Y, Kimura Y, Wang SM, Sharikadze N, et al. Knocking out sigma-1 receptors reveals diverse health problems. *Cell Mol Neurobiol* 2022;**42**:597−620.
48. Martina M, Turcotte ME, Halman S, Bergeron R. The sigma-1 receptor modulates NMDA receptor synaptic transmission and plasticity *via* SK channels in rat hippocampus. *J Physiol* 2007;**578**: 143−57.
49. Navarro G, Moreno E, Bonaventura J, Brugarolas M, Farré D, Aguinaga D, et al. Cocaine inhibits dopamine D2 receptor signaling *via* sigma-1−D2 receptor heteromers. *PLoS One* 2013;**8**:e61245.
50. Lee PT, Liévens JC, Wang SM, Chuang JY, Khalil B, Wu HE, et al. Sigma-1 receptor chaperones rescue nucleocytoplasmic transport deficit seen in cellular and *Drosophila* ALS/FTD models. *Nat Commun* 2020;**11**:5580.
51. Wang SM, Wu HE, Yasui Y, Geva M, Hayden M, Maurice T, et al. Nucleoporin POM121 signals TFEB-mediated autophagy *via* activation of SIGMAR1/sigma-1 receptor chaperone by pridopidine. *Autophagy* 2023;**19**:126−51.
52. Laurini E, Col VD, Mamolo MG, Zampieri D, Posocco P, Fermeglia M, et al. Homology model and docking-based virtual screening for ligands of the σ_1 receptor. *ACS Med Chem Lett* 2011;**2**: 834−9.

53. Banister SD, Manoli M, Doddareddy MR, Hibbs DE, Kassiou M. A σ_1 receptor pharmacophore derived from a series of *N*-substituted 4-azahexacyclo[5.4.1.0(2,6).0(3,10).0(5,9).0(8,11)] dodecan-3-ols (AHDs). *Bioorg Med Chem Lett* 2012;**22**:6053−8.
54. Gund TM, Floyd J, Jung D. Molecular modeling of sigma$_1$ receptor ligands: a model of binding conformational and electrostatic considerations. *J Mol Graph Model* 2004;**22**:221−30.
55. Laggner C, Schieferer C, Fiechtner B, Poles G, Hoffmann RD, Glossmann H, et al. Discovery of high-affinity ligands of sigma$_1$ receptor, ERG2, and emopamil binding protein by pharmacophore modeling and virtual screening. *J Med Chem* 2005;**48**:4754−64.
56. Oberdorf C, Schmidt TJ, Wünsch B. 5D-QSAR for spirocyclic sigma$_1$ receptor ligands by Quasar receptor surface modeling. *Eur J Med Chem* 2010;**45**:3116−24.
57. Zampieri D, Mamolo MG, Laurini E, Florio C, Zanette C, Fermeglia M, et al. Synthesis, biological evaluation, and three-dimensional *in silico* pharmacophore model for sigma$_1$ receptor ligands based on a series of substituted benzo[*d*]oxazol-2(^{3}H)-one derivatives. *J Med Chem* 2009;**52**:5380−93.
58. Meunier J, Hayashi T. Sigma-1 receptors regulate Bcl-2 expression by reactive oxygen species-dependent transcriptional regulation of nuclear factor κB. *J Pharmacol Exp Ther* 2010;**332**:388−97.
59. Maurice T, Privat A. SA4503, a novel cognitive enhancer with sigma$_1$ receptor agonist properties, facilitates NMDA receptor-dependent learning in mice. *Eur J Pharmacol* 1997;**328**:9−18.
60. Maurice T, Su TP, Privat A. Sigma$_1$ (σ_1) receptor agonists and neurosteroids attenuate β_{25-35}-amyloid peptide-induced amnesia in mice through a common mechanism. *Neuroscience* 1998;**83**:413−28.
61. Su TP, London ED, Jaffe JH. Steroid binding at sigma receptors suggests a link between endocrine, nervous, and immune systems. *Science* 1988;**240**:219−21.
62. Reyes ST, Deacon RMJ, Guo SG, Altimiras FJ, Castillo JB, van der Wildt B, et al. Effects of the sigma-1 receptor agonist blarcamesine in a murine model of fragile X syndrome: neurobehavioral phenotypes and receptor occupancy. *Sci Rep* 2021;**11**:17150.
63. Su TP, Wu XZ, Cone EJ, Shukla K, Gund TM, Dodge AL, et al. Sigma compounds derived from phencyclidine: identification of PRE-084, a new, selective sigma ligand. *J Pharmacol Exp Ther* 1991;**259**:543−50.
64. Monnet FP, Debonnel G, de Montigny C. *In vivo* electrophysiological evidence for a selective modulation of *N*-methyl-D-aspartate-induced neuronal activation in rat CA3 dorsal hippocampus by sigma ligands. *J Pharmacol Exp Ther* 1992;**261**:123−30.
65. Villard V, Espallergues J, Keller E, Vamvakides A, Maurice T. Anti-amnesic and neuroprotective potentials of the mixed muscarinic receptor/sigma$_1$ (σ_1) ligand ANAVEX2-73, a novel aminotetrahydrofuran derivative. *J Psychopharmacol* 2011;**25**:1101−17.
66. Lahmy V, Long R, Morin D, Villard V, Maurice T. Mitochondrial protection by the mixed muscarinic/σ_1 ligand ANAVEX2-73, a tetrahydrofuran derivative, in Aβ_{25-35} peptide-injected mice, a non-transgenic Alzheimer's disease model. *Front Cel Neurosci* 2015;**8**:463.
67. Lahmy V, Meunier J, Malmström S, Naert G, Givalois L, Kim SH, et al. Blockade of Tau hyperphosphorylation and Aβ_{1-42} generation by the aminotetrahydrofuran derivative ANAVEX2-73, a mixed muscarinic and σ_1 receptor agonist, in a nontransgenic mouse model of Alzheimer's disease. *Neuropsychopharmacology* 2013;**38**:1706−23.
68. Marrazzo A, Caraci F, Salinaro ET, Su TP, Copani A, Ronsisvalle G. Neuroprotective effects of sigma-1 receptor agonists against β-amyloid-induced toxicity. *Neuroreport* 2005;**16**:1223−6.
69. Goguadze N, Zhuravliova E, Morin D, Mikeladze D, Maurice T. Sigma-1 receptor agonists induce oxidative stress in mitochondria and enhance complex I activity in physiological condition but protect against pathological oxidative stress. *Neurotox Res* 2019;**35**:1−18.
70. Deane R, Wu Z, Sagare A, Davis J, Du Yan S, Hamm K, et al. LRP/amyloid β-peptide interaction mediates differential brain efflux of Aβ isoforms. *Neuron* 2004;**43**:333−44.
71. Zhao Z, Sagare AP, Ma Q, Halliday MR, Kong P, Kisler K, et al. Central role for PICALM in amyloid-β blood−brain barrier transcytosis and clearance. *Nat Neurosci* 2015;**18**:978−87.
72. Alon A, Schmidt H, Zheng S, Kruse AC. Structural perspectives on sigma-1 receptor function. *Adv Exp Med Biol* 2017;**964**:5−13.